*The 2016 World Congress on*
***Advances in Civil, Environmental, and Materials Research (ACEM16)***
*Jeju Island, Korea, August 28-September 1, 2016*

# Characterization of Creep Behavior of high Temperature P91 steel using Uniaxial Creep and Small Punch Tests

B. Deliktaş[1], M. Sönmez[2] and H.T Türker[3]

[1]*Department of Civil Eng., Uludag University, Gorukle, BURSA, 16069, Turkey*
[2]*Department of Civil Eng, Aksaray Üniversity, Aksaray 68100, Turkey*
[3]*Department of Civil Eng, İskenderun Technical University, İskenderun, 31034, Turkey*
[1)] *bdeliktas@uludag.edu.tr*

## ABSTRACT

The creep properties of P91 steels for high-temperature applications under high temperatures and pressures are extremely important. Therefore, in this paper, the characterization of uni-axial creep test data for P91 steels based on finite element analyses of small punch tests are performed. A set of uniaxial creep test data has been characterized in order to identify material model parameters using the evolutionary algorithms such as ant colony algorithm. The advantage of the proposed optimization approach is that parameter can be identified without any divergence in every case.

Finally, Finite Element (FE) analyses of small punch creep tests, using a damage mechanics based creep model, have been performed in order to accurately predict the behavior of the creep deformation and rapture behavior. The damage model was assessed by strain and deflection versus time graphs from uniaxial and SP creep tests for different stress and loads at 600˚C, respectively. A good agreement was found between the numerical and experimental curves for both test types.

## THEORETICAL BACKGROUND

### Constitutive Models for Creep Damage

P91 Steels exhibit a pronounced change in their microstructure as they are exposed to high-temperature service conditions, which determines their remnant creep life (Hyde and Sun, 2004, Hyde et al. 2007,2009, Rouse et al, 2013, Dyson, 2009).

---

[1] Professor
[2] Professor
[3] Professor

Under such conditions the creep deformation and rupture are important in the determination of limiting design factors such as strain histories, damage field evolution and lifetimes. Therefore, creep modeling has gained considerable importance in recent years in view of the growing needs to develop materials to be used in modern super critical and ultra-super critical power plants. These models generally attempt to characterize the full creep curve, including the primary, secondary and tertiary creep stages (Shan et al., 2008, Rouse et al., 2013, Sun et al., 2008,2013,2014).

Many studies showed that materials under high temperature deteriorate due to different mechanisms such as grain boundary slide, ductile void growth, diffusion of vacancies along the boundary and carbide precipitate coursing. Therefore, in this study multi-variable constitutive equations are proposed by Dyson, 1998,1999, 2002. This particular model includes the following mechanisms: cavitation damage from cavity nucleation and growth precipitate coursing, dislocation accumulation and strain hardening during primary creep. The form of the constitutive equations proposed for uniaxial conditions is given by the following set of equations.

$$\begin{aligned} \dot{\varepsilon} &= \boldsymbol{A}\sinh\left\{\frac{\boldsymbol{B}\,\boldsymbol{\sigma}(\mathbf{1}-\boldsymbol{H})}{(\mathbf{1}-\emptyset)(\mathbf{1}-\boldsymbol{w})}\right\} \\ \dot{\boldsymbol{H}} &= \frac{\boldsymbol{h}\,\dot{\boldsymbol{\varepsilon}}}{\boldsymbol{\sigma}}\left\{\mathbf{1}-\frac{\boldsymbol{H}}{\boldsymbol{H}^{*}}\right\} \\ \dot{\emptyset} &= \frac{\boldsymbol{K_C}}{\mathbf{3}}(\mathbf{1}-\emptyset)^{\mathbf{4}} \\ \dot{\boldsymbol{w}} &= \boldsymbol{DA}\sinh\left\{\frac{\boldsymbol{B}\,\boldsymbol{\sigma}(\mathbf{1}-\boldsymbol{H})}{(\mathbf{1}-\emptyset)(\mathbf{1}-\boldsymbol{w})}\right\} \end{aligned} \tag{1}$$

In the given set of equations above, the second term describes the primary creep due to initial strain hardening and the formation of dislocation microstructure (Kowalewski et al., 1994, Perrin et al., 1996, Othman et al., 1993, Hyhurst, 2003). In the third term of Eq. (8) the damage variable, $\emptyset$ is introduced to reflect the effects of precipitate coarsening that may restrict the deformation within grain interior (Dyson, 1998, Perrin, 1996,Tanner, 2013). This damage variable varies from 0 to 1. The fourth relation in Eq. (8) describes nucleation and growth of cavity that reduces the load bearing section and accelerate the creep damage. $w$ is the cavitation damage variable that varies from 0 to 0.3

**Non-linear parameter identification**

The main purpose of the parameter identification problems is to find the best design variable vector $\mathrm{x} \in \mathrm{X}$ by adjusting them until measured data (vector) $\mathrm{y} \in \Psi$ match the experimental or observed data set. . This kind of optimization problem is solved by meta-heuristic search optimization techniques such as Artificial Bee Colony Algorithm (Karaboga and Koyuncu, 2003, Sönmez, 2011) This algorithm can be incorporated into a parameter identification problem to obtain the function constants. In order to solve the constitutive equations given in Eq. (1) by using Euler forward integration scheme, the equations can be rewritten in the finite difference format as:

$$\begin{aligned}
\boldsymbol{\varepsilon_{i+1}} &= \boldsymbol{\varepsilon_i} + \boldsymbol{\Delta t\, A \sinh}\left\{\frac{\boldsymbol{B\,\sigma\,(1-H_i)}}{\boldsymbol{(1-\emptyset_i)(1-w_i)}}\right\} \\
\boldsymbol{H_{i+1}} &= \boldsymbol{H_i} + \frac{\boldsymbol{h\,(\varepsilon_{i+1}-\varepsilon_i)}}{\boldsymbol{\sigma}}\left\{\boldsymbol{1-\frac{H_i}{H_i^*}}\right\} \\
\boldsymbol{\phi_{i+1}} &= \boldsymbol{\phi_i} + \boldsymbol{\Delta t}\,\frac{\boldsymbol{K_C}}{\boldsymbol{3}}\boldsymbol{(1-\emptyset_i)^4} \\
\boldsymbol{\omega_{i+1}} &= \boldsymbol{\omega_i} + \boldsymbol{\Delta t\, D\, A \sinh}\left\{\frac{\boldsymbol{B\,\sigma(1-H_i)}}{\boldsymbol{(1-\phi_i)(1-\omega_i)}}\right\}
\end{aligned} \qquad \textbf{(2)}$$

At the first step on the construction of the strain-time curve for different stress level, the initial $H_0$, $\phi_0$ and $\omega_0$ given in Eq. (2) are set to zero at $t = 0$, then the forward finite difference methods are performed for each stress levels until strains ($\varepsilon_i$) reach maximum level which is obtained from experiments. The experimental strain-time curves are not evenly spaced intervals of the time variable; while, the estimated strain-time curves are evenly spaced. Hence, both experimental and calculated strains must be known at current time. In order to convert the unevenly spaced experimental data to evenly spaced interval, the linear interpolation technique has been employed. Then the objective function which is used to determine the optimum parameters, is calculated as:

$$\mathbf{E} = \sum_{\boldsymbol{j=1}}^{\boldsymbol{m}} \sum_{\boldsymbol{t=1}}^{\boldsymbol{t_{max}}} \left( \frac{\boldsymbol{\varepsilon_{exp}^{j}(t_i) - \varepsilon_{cal}^{j}(t_i)}}{\boldsymbol{\varepsilon_{exp}^{j}(t_{max})}} \right)^{\mathbf{2}} \qquad \textbf{(3)}$$

where $\varepsilon_{exp}^{j}(t_i)$ and $\varepsilon_{exp}^{j}(t_i)$ are an experimental strain and calculated strain at time $t_i$, respectively. $m$ is used for the number of stress level; $t_{max}$ is for the maximum time for stress level $j$. The ABC algorithm is used to minimize Eq. (3) by changing the six uniaxial constants, *A, B, h, H*, Kc* and *D.*

**Material Constants of Dyson and McLean Constitutive Equations**

The six uniaxial constants, *A, B, h, H*, Kc* and *D*, can be determined by fitting a number of uniaxial strain–time curves obtained from creep tests. For given temperature of uniaxial strain–time relationship, governed by Eqs. (2). The material constant sets, determined from the proposed optimization procedure are shown in Table-1.

**Table 1: Material constants of Dyson and MacLean Model for P91 Steel (stress(MPa), Time(Hr) )**

| Material P91 | A | B | h | $H^*$ | $K_c$ | $D$ |
|---|---|---|---|---|---|---|
| Set1 | $3.0891\times10^{-10}$ | $1.07287\times10^{-1}$ | $7.64505\times10^{3}$ | $1.87373\times10^{-1}$ | $1.0\times10^{-7}$ | 2.52243 |

Figure 1 show the experimental and fitted uniaxial creep strain curves for P91 steel at 600 $^{o}$C, in a stress range 135,145 and 155 MPa, for the Dyson-McLean creep equation, using material data sets given in Table 1.

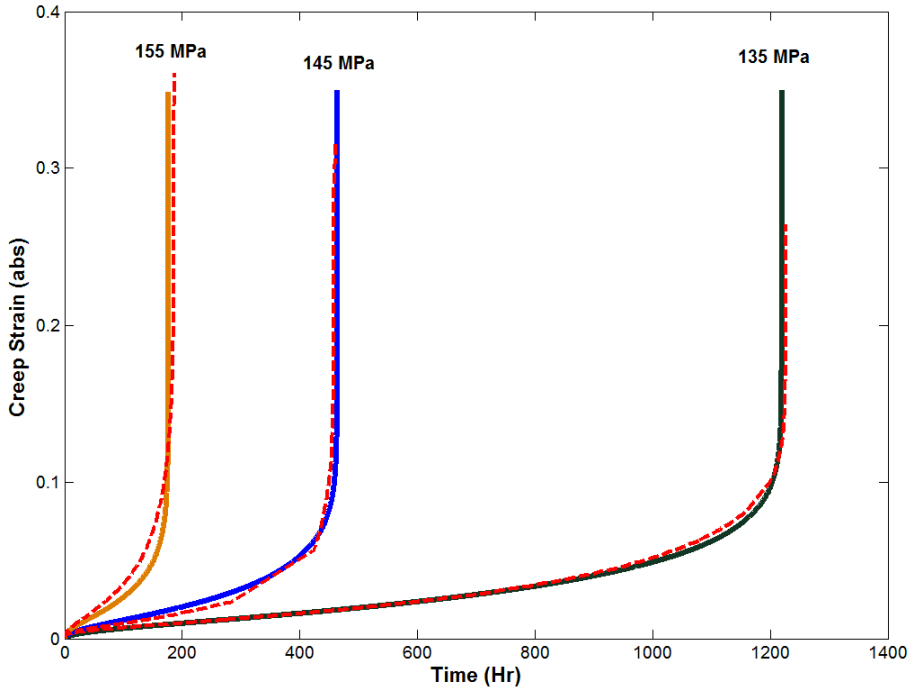


**Fig. 1. Fitted uniaxial creep strain curves to the experimental data of the p91 steel at 600 $^{o}$C under constant stresses (Solid lines: Model, Dotted lines: Experiments(Blagoeva et al., 2009, Deliktas et al., 2014))**

As one can see that the fitted curves calculated using four different optimized data sets given in Table 1 are agreed very well with experimental data, indicating that the identified material creep constants *A, B, h, H*, Kc* and *D* in Eq. (13) can accurately represent the uniaxial behavior of the material. These results indicate that the proposed optimization technique is adequate for finding the parameter set that describes the material behavior.

## SIMULATION OF SMALL PUNCH TEST

In this section the small punch test is simulated using the Dyson and Mclean constitutive model in order to better understand what is happening during small punch creep testing and accurately predict the behavior of the creep deformation and rupture behavior of the P91 steel. FE model is constituted as 2D axisymmetric in order to reduce the computation time (Figure 2). Geometrically nonlinear steady state finite element setup and solution is followed.

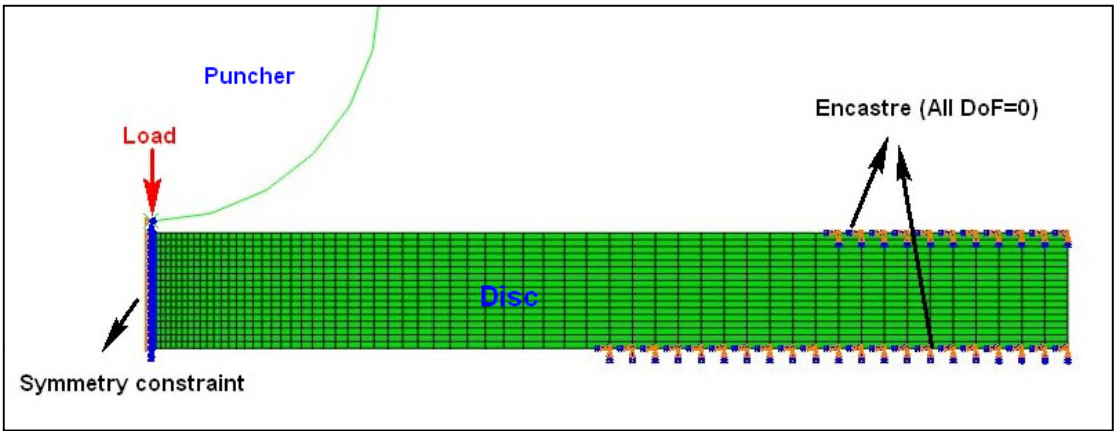


**Fig. 2 FE model of SP creep test**

As seen in Figure 2, the disc was clamped at the edges in contact with the upper and lower die. The punch and the dies are modeled as rigid bodies. The disc is meshed in a non-uniform pattern so that the mesh density is higher towards the area of interest; center of the disc where the deformation is much bigger. As mentioned before in some cases it is not possible to have available the large amount of material required for a conventional cylindrical specimen. Therefore, the material parameter set determined from the conventional uniaxial set may not be used directly in simulation of any structural components that operate under high temperature and stress conditions, where the creep deformation and rupture are important in the determination of limiting design factors.

Therefore, in this study, uniaxial test data used in conjunction with optimization procedure to determine material model set. Then, these data set is used as starting reference data to recalibrate material data set using SPT. The determined new parameter set from the corresponding optimization procedure is given Table 2.

**Table 2: Material constants of Dyson and Maclean for P91 Steel stress(MPa) Time(Hr)**

| Material P91 | A | B | h | $H^*$ | $K_c$ | $D$ |
|---|---|---|---|---|---|---|
| | $3.0891 \times 10^{-10}$ | $0.93055 \times 10^{-1}$ | $9.64505 \times 10^{3}$ | $1.37373 \times 10^{-1}$ | $1.512 \times 10^{-3}$ | 0.45243 |

With the resulting set of constitutive constants given in Table 2 the experimental data is fitted by calculated curves using the creep damage constitutive equations (Figure 3).

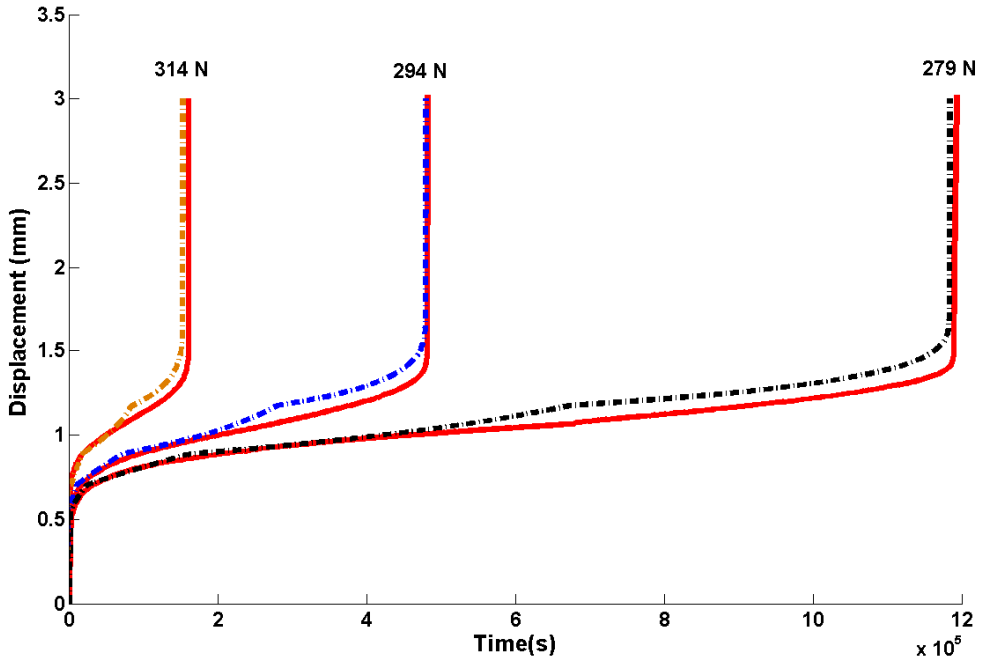


**Fig. 3. Fitted SPT displacement curves to the experimental data of the p91 steel at 600 $^{o}$C under constant loads of 279N, 294N, and 314 N respectively. (Dotted lines: Model, Solid lines: Experiments(Blagoeva et al., 2009, Deliktas et al., 2014))**

Figure 3 shows that the calibrated constitutive constants fit closely the calculated curves to the experimentally observed displacement time curves under constant loads of 276N, 294N, and 314N, respectively.

In order to understand the behavior of the creep deformation and rupture of the P91 steel under small punch creep testing, various responses of the small punch simulation underneath the puncher with the constant load of 314N, such as the distributions of von Mises stress, equivalent plastic strain, equivalent creep strain, and the damage state variables have been evaluated by looking at their counter plots resulting from FEM analyses.

Figure 4 depicts the counter plots of equivalent plastic strain counter of SPC specimen obtained from the finite element analysis of small punch creep testing**.**

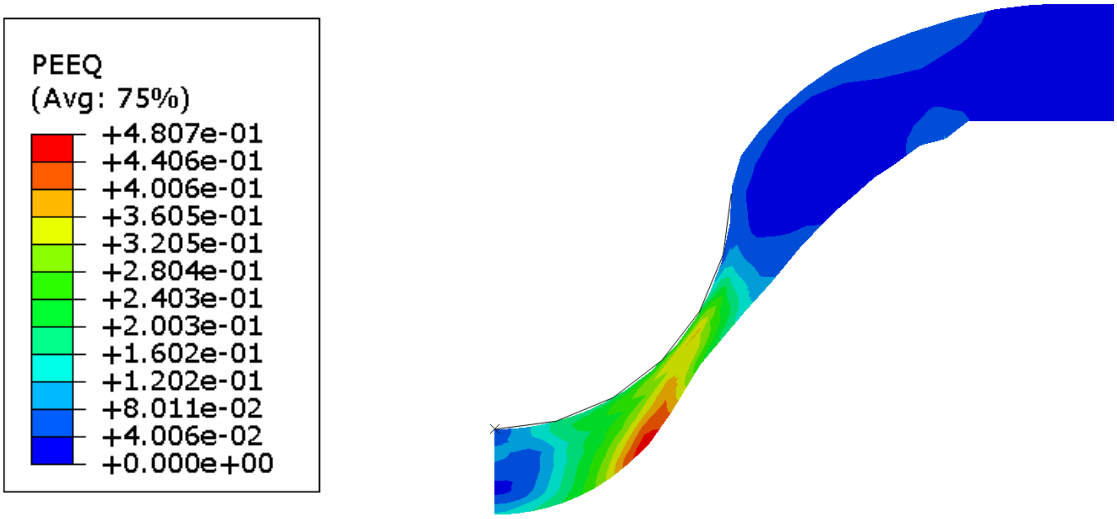


**Fig: 4 Equivalent plastic strain counter plot and deformation shape**

It is clearly seen that plastic deformation localize as the creep time increases. The localized region is located at the bottom surface in the central area of the specimen. In the following figure equivalent creep strain counter with its deformation shape obtained from fine element analysis is presented (Figure 5).

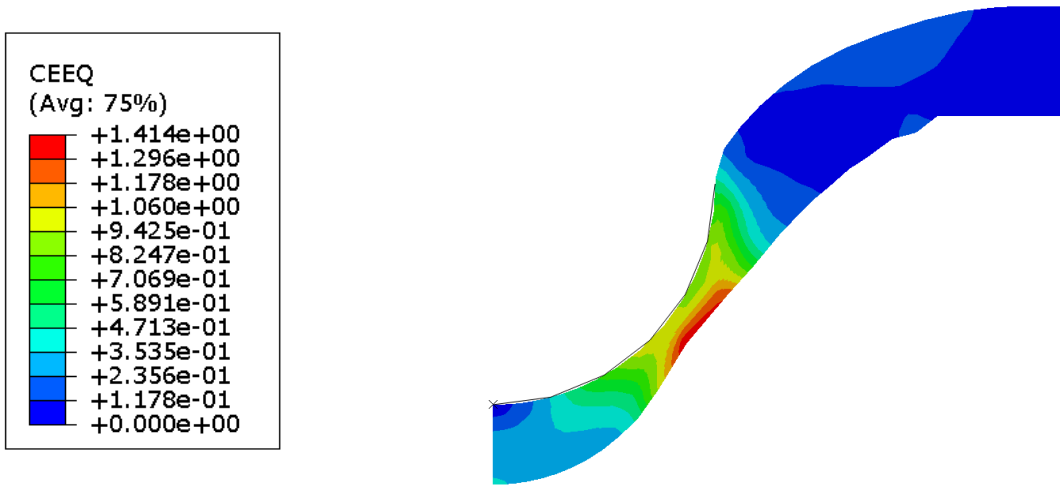


**Fig: 5. Equivalent creep strain counter plot and deformation shape**

In this figure accumulated creep strain moves further upward as opposed the equivalent plastic strain counter. At the localized equivalent plastic strain region on can observe that necking occurs. This is an expected deformation mechanism since the damage state variable, which is attributed to the effects of cavitation damage is governed by accumulated creep strain.
Figure 6 shows the counter plots of damage state variables due to precipitate coursing and cavity nucleation and growth, respectively.

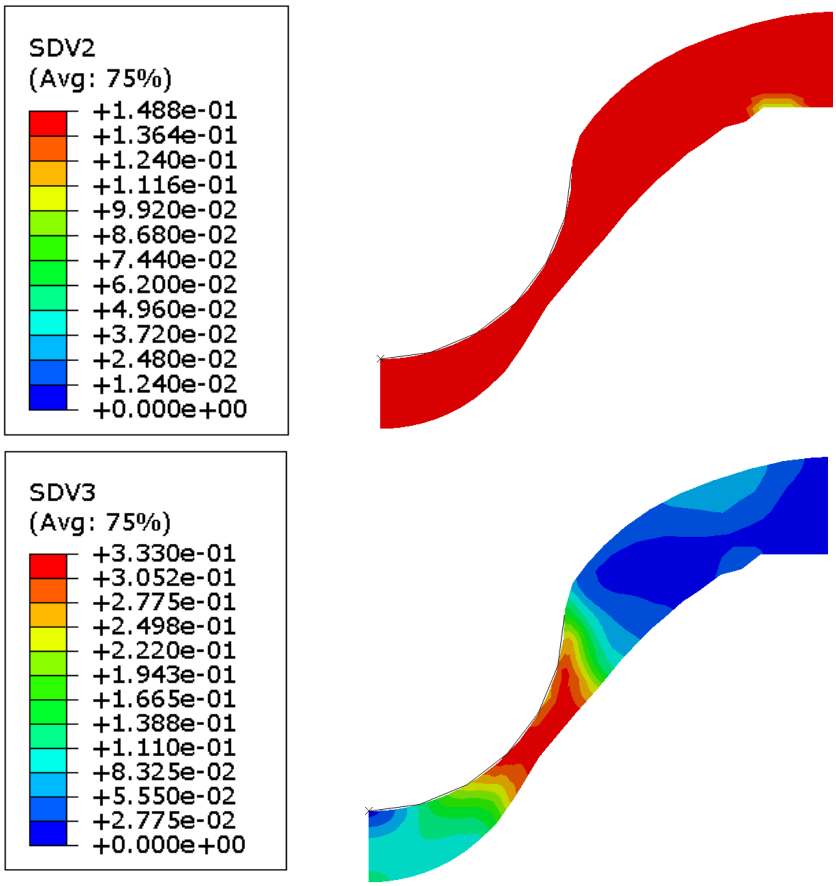


**Fig: 6** Damage variables counter plot and deformation shape

As the creep time increases the value of the creep damage in the material increases and some elements exceed damage threshold value start to fail gradually. As a result of these failed elements, localized necking deformation occurs at location around the bottom surface of the contact area between the puncher and the specimen.

## CONNCLUSION

The creep properties and the behavior of the P91 steel that are widely used for welded steam pipes in the construction of power plant components are determined by means of uniaxial and small punch experiments in conjunction with finite element analyses. First material characterization in terms of identifying constitutive constants are performed using both uniaxial data and SPT data sets following the proposed optimization procedure in this study. Finally creep deformation and rupture behavior of the SPT are predicted by finite element analyses. The proposed optimization procedure is reliable and efficient for identifying the constitutive constants using the uniaxial and SPT data sets. However, it is concluded that the material parameter set determined only from the conventional uniaxial set may not be adequate to use directly in simulation of any structural components that operate under high temperature and

stress conditions. Therefore, uniaxial test data should be recalibrated using material data set obtained from SPT.

## REFERENCES

Blagoeva, D.T. and R.C. Hurst,(2009), *Application of the CEN (European Committee for Standardization) small punch creep testing code of practice to a representative repair welded P91 pipe.* Materials Science and Engineering a-Structural Materials Properties Microstructure and Processing, 510-11: p. 219-223.

Deliktas B. Gülçimen, B. Hahner P., (2014), Thermoplasticity coupled damage model for predicting behavior of P91 steel during small punch creep testing, 3th International Workshop on Physics Based Material Models and Experimental Observation, Special Focus: Plasticity and Creep, 2-4,June,İzmir, Turkey

Dyson, B.F.,(1998), *Physically-Based Models of Metal Creep for Use in Engineering Design.* Journal of Metals, 40(7): p. A35-A35.

Dyson, B.F.,(1999), *Creep mechanism transition in precipitation strengthened alloys: Theory and validation.* Creep Behavior of Advanced Materials for the 21st Century, p. 3-12.

Dyson, B.F., (2002), *Modelling creep rupture ductilities and lifetimes in a commercial aluminium alloy.* Creep Deformation: Fundamentals and Applications, p. 309-318.

Dyson, B.F.,(2009), *Microstructure based creep constitutive model for precipitation strengthened alloys: theory and application.* Materials Science and Technology, 25(2): p. 213-220.

Dyson, B.F. and M. McLean, (1998), *Microstructural evolution and its effects on the creep performance of high temperature alloys.* Microstructural Stability of Creep Resistant Alloys for High Temperature Plant Applications, p. 371-393.

Hyde, T.H. and W. Sun,(2004), *High temperature behaviour of materials and components under creep conditions.* Advances in Experimental Mechanics, 1-2: p. 25-34.

Hyde, T.H., W. Sun, and A.H. Yaghi,(2007), *Structural integrity analysis of power plant welds subjected to high temperature creep.* Engineering Structural Integrity: Research, Development and Application, Vols 1 and 2, p. 735-739.

Hyde, T.H., et al.,(2009), *Some issues on structural integrity analysis of P91 welds in power plants subjected to high temperature creep*.* Fatigue & Fracture of Engineering Materials & Structures, 32(11): p. 926-935.

Karaboga, N. and C.A. Koyuncu,(2005), *Differential evolution algorithm for designing optimal adaptive linear combiners.* Advances in Artificial Intelligence, 3809: p. 1063-1067.

Kowalewski, Z.L., D.R. Hayhurst, and B.F. Dyson,(1994), *Mechanisms-Based Creep Constitutive-Equations for an Aluminum-Alloy.* Journal of Strain Analysis for Engineering Design, 29(4): p. 309-316

Perrin, I.J. and D.R. Hayhurst,(1996), *Creep constitutive equations for a 0.5Cr-0.5Mo-0.25V ferritic steel in the temperature range 600-675 degrees C.* Journal of Strain Analysis for Engineering Design, 31(4): p. 299-314.

Perrin, I.J. and D.R. Hayhurst,(1999), *Continuum damage mechanics analyses of type IV creep failure in ferritic steel crossweld specimens.* International Journal of Pressure Vessels and Piping, 76(9): p. 599-617.

Rouse, J.P., W. Sun, and T.H. Hyde,(2013), *The effects of scoop sampling on the creep behaviour of power plant straight pipes.* Journal of Strain Analysis for Engineering Design, 48(8): p. 494-511.

Rouse, J.P., et al.,(2013), *Comparative assessment of several creep damage models for use in life prediction.* International Journal of Pressure Vessels and Piping, 108: p. 81-87.

Shan, J.H., X. Ling, and Z.M. Qian, (2008), *Residual life assessment of in-service high temperature components by small punch creep test.* Proceedings of the Asme Pressure Vessels and Piping Conference 2007, Vol 9, p. 427-432.

Sonmez M., (2011), A*rtificial Bee Colony algorithm for optimization of truss structures,* Applied Soft Computing, 11(2): p. 2406-2418.

Sun, W., A.A. Becker, and T.H. Hyde,(2013), *Materials and structural assessment under high temperature creep and fatigue.* Materials Research Innovations, 17(5): p. 298-299.

Sun, W., A.A. Becker, and T.H. Hyde, (2014), *Creep deformation, damage and thermal-mechanical fatigue analysis of high temperature materials and welds.* Materials Science and Technology, 30(1): p. 4-5.

Sun, W., T.H. Hyde, and S.J. Brett, (2008), *Application of impression creep data in life assessment of power plant materials at high temperatures.* Proceedings of the Institution of Mechanical Engineers Part L-Journal of Materials-Design and Applications, 222(L3): p. 175-182.

Tanner, D.W.J., W. Sun, and T.H. Hyde, (2013), *Cross-Weld Creep Comparison of Power Plant Steels CrMoV, P91 and P92.* Journal of Pressure Vessel Technology-Transactions of the Asme, 135(2).